Int. J. Electrochem. Sci., 14 **(2019)** 4903 – 4916, doi: 10.20964/2019.05.16

International Journal of
ELECTROCHEMICAL
SCIENCE
www.electrochemsci.org

Effect of dodecylbenzenesulphonate on Electrocatalytic Activity of NiOx Nanoparticles for glucose oxidation

Mohamed S. Mohamed Ahmed[1,2*], *Zeinab A. Abdallah*[1,2], *Mahmoud M. Saleh*[1,2*]

[1]Chemistry Department, College of Science, King Faisal University, Al-Hassa, KSA
[2]Department of Chemistry, Faculty of Science, Cairo University, Giza, Egypt
[*]E-mail: mzidane@kfu.edu.sa, mahmoudsaleh90@yahoo.com

Received: 29 September 2018 / *Accepted:* 5 February 2019 / *Published:* 10 April 2019

The impacts of addition of organic compound (anionic surfactant) dodecylbenzenesulphonate (DBS) on the electrodeposition of nickel oxide (NiO_x) nanoparticles and on the electrocatalytic oxidation of glucose from alkaline solution are studied. NiO_x nanoparticles are electrodeposited on the surface of a glassy carbon (GC) electrode in the presence and absence of the DBS. Cyclic voltammetry (CV), field emission-scanning electron microscopy (SEM) and energy dispersive X-ray spectroscopy (EDX) are used for characterization of the above electrodes. The peak current of the redox couple Ni(II)/Ni(III) increases with the [DBS] before it decreases at [DBS] > 1×10^{-4} M. The electrocatalytic activity of the NiO_x/GC electrode towards the electrochemical oxidation of glucose is affected by the same manner. An attempt to correlate this electrocatalytic enhancement with the addition of the DBS is introduced. Optimum concentration of the DBS is obtained that gives the best enhancement in the electrochemical and electrocatalytic properties.

Keywords: Surfactant, Nickel, Nanoparticles, Electrocatalysis, Glucose

1. INTRODUCTION

Surface active molecules or surfactants have long been known for their importance from technological and academic point of view. It has serious impacts on electrochemical systems which has been documented several times [1–4]. The unique chemical and structural features of the surfactants such as the hydrophilic moiety of the molecule (the polar head group) which may be positive, negative, neutral or zwitterionic and the hydrophobic moiety (the tail) that consists of one or more hydrocarbon chains, usually with 6–22 carbon atoms. Two important properties of surfactants are well known. Adsorption at interface and aggregation into supramolecular structures are advantageously used in electrochemistry. Surfactants are able to modify and control the properties of electrode/electrolyte

interfaces. In this context, surfactants in general have been used for different applications which include: electroplating [5], fuel cells [6], electrocatalytic and energy conversion systems [7-10]. In electrocatalysis, surfactant can be added in situ with the electrochemical reactant [10, 11] or can be used during the electrodeposition of the catalyst [12, 13]. For instance, an anionic surfactant was used in the electrodeposition bath of MnO_2 and obtained a significant increase of the supercapacitance performance of MnO_2 nanoparticles modified electrode [14]. On the other hand, some authors used surfactant as an addition to the electrochemical reaction bath to enhance the electrochemical reaction of certain catalyst [15].

Ni and Ni-based electrocatalysts (e.g., NiO) represents an important category of electrocatalysts that have been used in many technological applications. Most of these applications rely on the properties of the redox couple Ni(II)/Ni(III). These applications can be from electrocatalysis to supercapacitor and from battery to sensors [16-23]. The electrochemical preparation, in specific, is mostly achieved on glassy carbon electrodes. The morphology of the used NiO_x nanoparticles affects the electrochemical performance of the modified electrode by those nanoparticles [24,25]. Many studies on glucose oxidation via different metal oxides with different sizes (bulk and nano-scale) including nickel oxide have been reported [26-30]. It is notable that nickel and nickel oxides display good electrocatalytic properties in aqueous solutions [31-33].

In the present work we aimed to study the impacts of addition of anionic surfactant (DBS) during the NiO_x electrodeposition in the electroplating bath on the GC surface and on the electrochemical characteristic of the GC/NiO_x. The impacts of different concentrations of the DBS added in the Ni deposition bath will be studied using surface analysis (FE-SEM) and electrochemical (CV) techniques. The electrocatalytic oxidation of glucose from alkaline medium will be used as a probe reaction to evaluate the impacts of the above factors on the electrocatalytic properties of the fabricated NiO_x nanoparticles.

2. EXPERIMENTAL

All used materials are purchased from Sigma-Aldrich and have been utilized as obtained. All solutions were prepared using bi-distilled water.

2.1. Measurements

Conventional electrochemical cell has been utilized for the experimental study. This consists of a platinum wire and an Ag/AgCl/KCl (sat.) as the counter and reference electrode, respectively. Electrochemical measurements were performed using Gamrypotentiostat/galvanostat supported with Gamry electrochemical analysis technique. All potentials will be presented with respect to this reference electrode. The working electrode was a glassy carbon (d = 3.0 mm). It was cleaned by mechanical polishing with aqueous slurries of successively finer alumina powder (down to 0.06 μm)

then washed thoroughly with second distilled water. Scanning electron microscope (SEM) images were taken using field emission scanning electron microscope, FE-SEM (FEI, QUANTA FEG 250).

2.2. Electrode modification

GC modification with NiO_x was achieved as the following: the potentiostatic deposition of metallic nickel on the working electrode (i.e., GC, d = 3 mm) from an aqueous solution of 0.1 M acetate buffer solution (ABS, pH = 4.0) containing 1 mM $Ni(NO_3)_2 \cdot 6H_2O$ with and without the addition of different concentration of DBS by using a fixed potential of −1.0 V. Second is the passivation of the obtained Ni surface in 0.1 M phosphate buffer solution (PBS, pH = 7) by potential cycling in the range of −0.5 to 1 V for 10 cycles at a scan rate of 200 mV/s. Then activation for 20 cycles in 0.5 M NaOH solution in the potential range −0.2 to 0.6 V.

3. RESULTS AND DISCUSSION

3.1. Electrochemical study

As discussed in the experimental section, the GC/NiO_x was prepared in the absence and presence of the DBS in the Ni-deposition bath. Two electrodes have been prepared, GC/NiO_x and $GC/NiO_{x\text{-}An}$. In the first one, NiO_x was fabricated such that no surfactant was added to the Ni deposition bath while in case of the other electrode ($GC/NiO_{x\text{-}An}$), the NiO_x nanoparticles was fabricated in different DBS concentrations during the Ni deposition bath in the acetate buffer (pH = 4). In all cases, a fixed amount of charge (Q = 25 mC, i.e., 5 min deposition) was passed in order to obtain an equal Ni loading upon deposition. In such a case, different time periods will be used to obtain such amount of charge. Table 1 shows the time period, t_{dep} required for the deposition or passing 25 mC at different DBS concentrations.The table reveals that t_{dep} decreases with the [DBS] before it increases at [BDS] > 1×10^{-4} M. It implies that the rate of electrodeposition of Ni is faster in presence of DBS ([DBS] < 1×10^{-4} M) than in absence of the DBS. The conductivity of the DBS solution increases linearly with the [DBS] up to it critical micelle concentration, CMC. The cited value of the CMC of the DBS at similar conditions is ~ 5×10^{-4} M [34].

Table 1. Time required (t_{dep}) for electrodeposition of fixed amount of Ni (Q = 25 mC in all cases) on GC using different concentrations of DBS in the nickel bath.

[DBS]/ M	0	10^{-6}	5×10^{-6}	10^{-5}	5×10^{-5}	10^{-4}	5×10^{-4}	10^{-3}
t_{dep} **/ s**	300	223	201	189	173	162	307	332

Figure 1 depicts CV responses of GC/NiO_x and GC/$NiO_{x\text{-}An}$ in 0.5 M NaOH (blank) at scan rate of 100 mV s^{-1}. Note that the GC/NiO_x and GC/$NiO_{x\text{-}An}$ are the NiO_x modified GC electrode where NiO_x was prepared in absence and presence of DBS, respectively. Curve "a" shows the CV response of the GC bare electrode and it appears to have no features at the used potential range. Curve "b" shows that of GC/NiO_x and it reveals the peaks of the redox couple Ni(II)/Ni(III) conversion. The GC/$NiO_{x\text{-}An}$ was prepared in different concentrations of the DBS that added during the Ni deposition in the range between 1×10^{-6} M DBS (curve c) to 1×10^{-3} M DBS (curve i). The CVs shows the normal features that characterize the redox couple of $Ni(OH)_2$/NiOOH (*i.e.*, Ni^{2+}/Ni^{3+}) according to the reaction below;

$$Ni(OH)_2 + OH^- \leftrightarrow NiOOH + H_2O + e^- \quad (1)$$

All CVs reveal the common redox peaks of the conversion, $Ni(OH)_2 \leftrightarrow$ NiOOH but with a height dependent on the DBS concentration. As the DBS concentration increases, the peak current of both the anodic and cathodic sweeps increases before it decreases at [DBS] > 1×10^{-4} M (see Fig. 1). Also, a negative shift in the onset potential, E_{onst} of the redox couple is observed. Figure 2 (curve A) shows the relation of peak current, I_p of the anodic sweep of the Ni(II)/Ni(III) redox conversion as a function of the [DBS] concentration. The peak current increases up to [DBS] = 1×10^{-4} M after which I_p decreases to lowers values. At these high concentrations, the DBS tends to form micelles rather than adsorbing on the electrode surface.

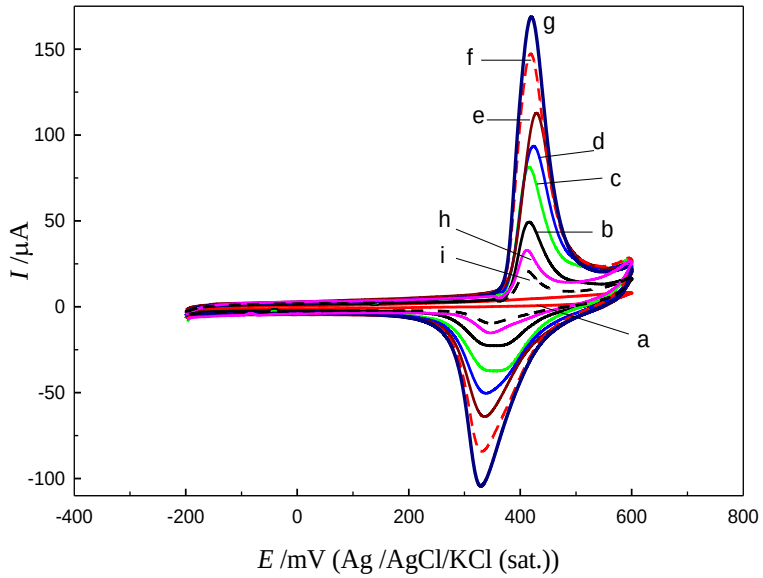

Figure 1. CV responses of GC/NiO_x and GC/$NiO_{x\text{-}An}$ in 0.5 M NaOH (blank) at scan rate of 100 mV s^{-1}. Curves: (a) GC, (b) GC/NiO_x (without DBS) and (c-i) GC/$NiO_{x\text{-}An}$ where the [DBS] is 0, 1×10^{-6}, 5×10^{-6}, 1×10^{-5}, 5×10^{-5}, 1×10^{-4}, 5×10^{-4}, 10^{-3}, respectively.

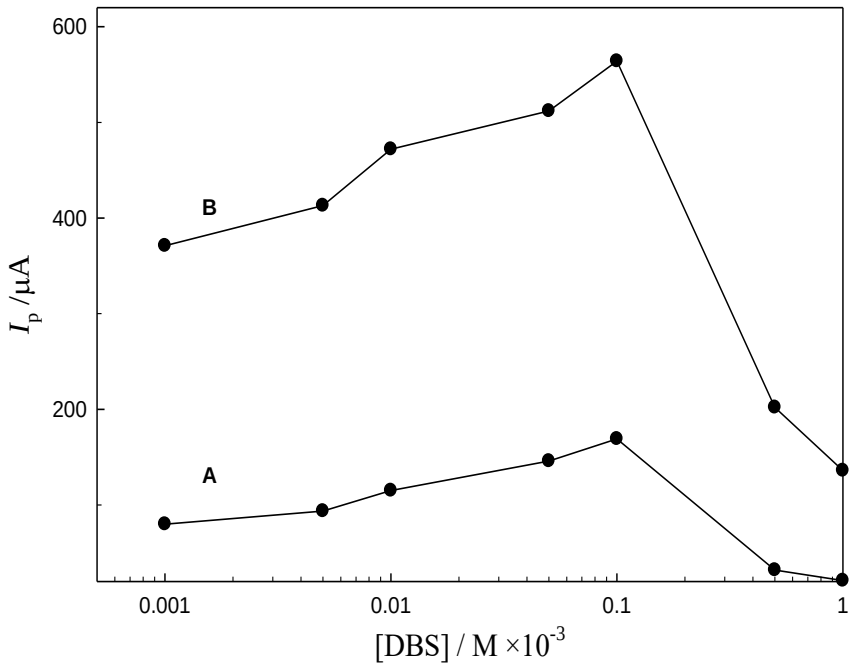

Figure 2A. The relation of peak current, I_p of the Ni(II)/Ni(III) redox conversion as a function of the [DBS] in blank (data taken from Fig. 1). B: The relation of the I_p of glucose oxidation as a function of the [DBS] (data taken from Fig. 4).

The reversibility of the $Ni(OH)_2$/NiOOH couple can be illustrated by estimating the CV parameters of the above redox couple at different conditions for the GC/NiO_x and GC/$NiO_{x\text{-}An}$ electrodes. Table 2 lists these parameters at different [DBS] concentrations. Those parameters are; the anodic and cathodic peak potentials (E_{pa} and E_{pc}, respectively), anodic and cathodic peak currents (I_{pa} and I_{pc}, respectively), the peak separation, ΔE_p and the ratio of the peak anodic current to the peak cathodic current.

Table 2. CV parameters of GC/$NiO_{x\text{-}An}$ in 0.5 M NaOH at different [DBS] concentrations at scan rate 100 mV s^{-1}. The GC/$NiO_{x\text{-}An}$ was prepared by adding different concentrations of DBS in the Ni deposition bath.

Electrode	**[DBS]/ M**	E_{pa}/ mV	E_{pc}/ mV	ΔE_p/ mV	I_{pa}/ μA	I_{pc}/ μA	I_{pc}/I_{pa}
GC/$NiO_{x\text{-}An}$	0	415	350	65	50	21.9	0.43
	10^{-6}	420	347	73	82.2	36.5	0.44
	5×10^{-6}	425	342	83	91.2	49	0.54
	10^{-5}	430	332	98	113.5	63.5	0.56
	5×10^{-5}	417	327.5	85	146	83.3	0.57
	10^{-4}	420	325	95	170	104	0.62
	5×10^{-4}	412	342.6	69	30	16.7	0.56
	10^{-3}	410	345	65	21	10.4	0.50

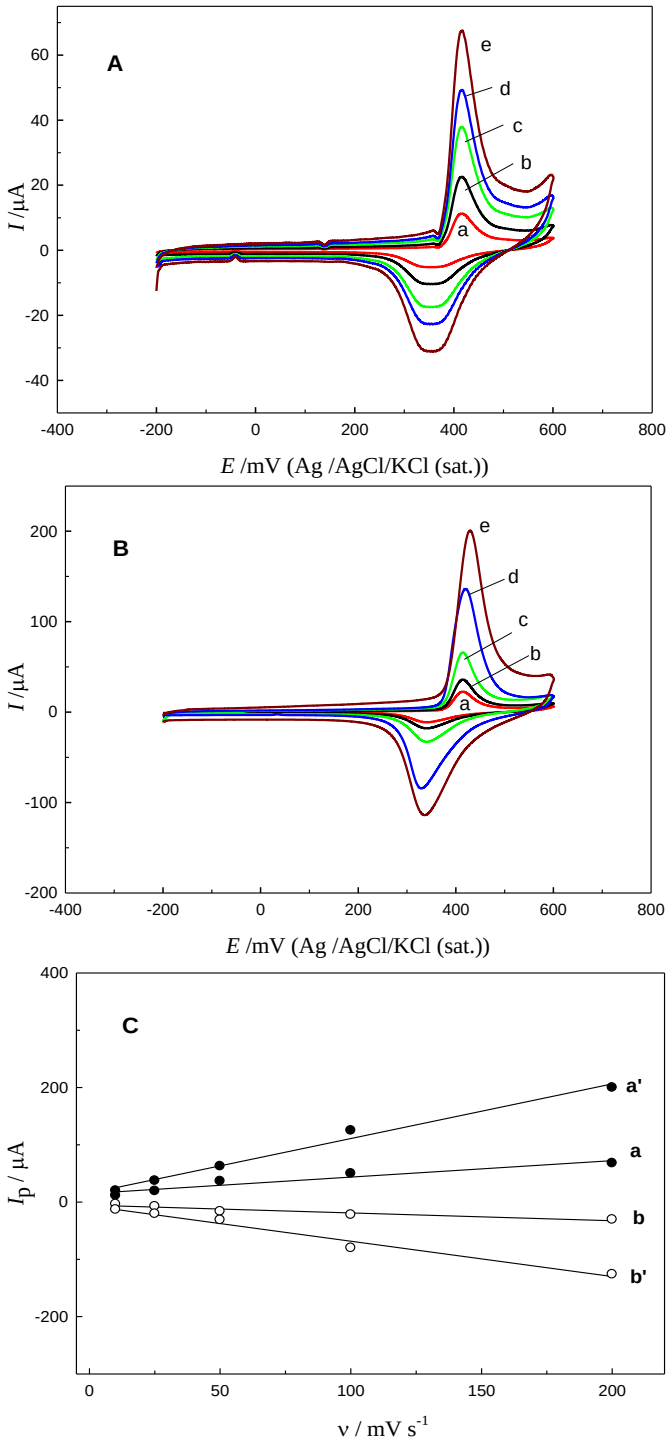

Figure 3. The effects of potential scan rate, ν on the CV response of the GC/NiO_x (A) and GC/$NiO_{x\text{-}An}$ (B) electrodes in blank 0.5 M NaOH solution (ν: 10. 25, 50, 100 and 200 mV s^{-1}). (C) A plot of the peak current for both anodic and cathodic sweeps, I_p with the scan rate, ν (a, b for GC/$NiO_x$and a', b'for GC/$NiO_{x\text{-}An}$).

The results in Table 2 demonstrate that ΔE_p are almost equal in all cases with an average value of 85 mV. Meanwhile, the ratio I_{pc}/I_{pa} is much closer to unity in case of GC/$NiO_{x\text{-}An}$ at [DBS] = 1×10^{-4} M. This demonstrates that the reversibility in case of the GC/$NiO_{x\text{-}An}$ is improved on adding the DBS

during the Ni deposition process and is in agreement with the above obtained results. The data in Table 1 and 2 and in Fig. 2 point to that an optimum DBS concentration of 1×10^{-4} M is concluded.

The effects of potential scan rate, ν on the CV response of Ni^{2+}/Ni^{3+} redox couple of the GC/NiO_x and GC/$NiO_{x\text{-}An}$ (electrodeposited in 1×10^{-4} M DBS) electrodes in blank 0.5 M NaOH solution are shown respectively in Fig. 3A,B.The peak current increases with the scan rate in both cases. A plot of the peak current for both anodic and cathodic sweeps, I_p with the scan rate, ν gives a straight line in both cases (Fig. 3C) pointing to a surface-confined process in both electrodes. It is concluded that there is no change in the nature of the redox the $Ni(OH)_2 \leftrightarrow$ NiOOH couple on both electrodes.

3.2. Glucose oxidation

In this section the impacts of the above enhancement of the electrochemical characteristics of the GC/NiO_x on its electrocatalytic activity towards electrooxidation of glucose from alkaline solution are studied.

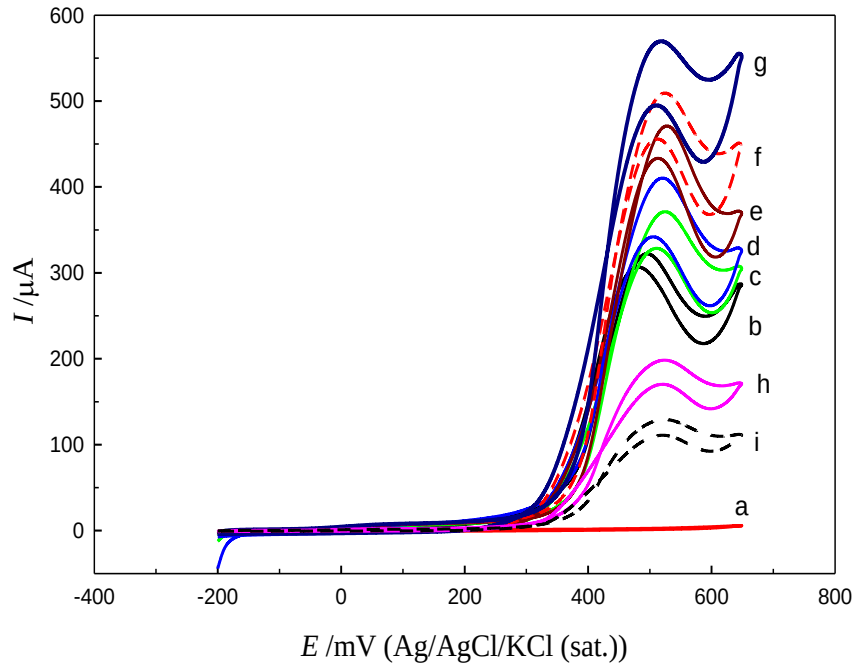

Figure 4. CV responses of GC/NiO_x and GC/$NiO_{x\text{-}An}$ in 0.5 M NaOH containing 20 mM glucose at scan rate of 100 mV s^{-1}. Curves: (a) GC, (b) GC/NiO_x (without DBS) and (c-i) GC/$NiO_{x\text{-}An}$ where the [DBS] is 0, 1×10^{-6}, 5×10^{-6}, 1×10^{-5}, 5×10^{-5}, 1×10^{-4}, 5×10^{-4}, 10^{-3}, respectively.

Figure 4 shows CV responses for glucose oxidation on GC/NiO_x and GC/$NiO_{x\text{-}An}$ using 20 mM glucose in 0.5 M NaOH. The GC/$NiO_{x\text{-}An}$ was prepared by using different concentrations of DBS (CVs from "c" to "i"). The peak current of the glucose oxidation increases with the DBS concentration before it decreases at [DBS] > 1×10^{-4} M (see Fig. 2B). The trend of the I_p with the [DBS] in Fig. 2B in presence of glucose is coincidence with that found in Fig. 2A in the blank. It means that the

enhancement of the $Ni(OH)_2 \leftrightarrow NiOOH$ accompanying by an enhancement of the glucose electrooxidation. This confirms the rule of the NiOOH species on the mediation of glucose electrooxidation. It is worthy to mention that a fixed amount of charge (25 mC) is used in the nickel deposition on the underlying electrode for all cases. Hence, the increase in the peak current of glucose oxidation is not attributed to a difference in the NiO_x amount but rather to the modification upon addition of the anionic surfactant in the nickel bath.Figure 5 depicts SEM images of the GC/NiO_x (A) and GC/$NiO_{x\text{-}An}$ (B) and the EDX chart. The GC/$NiO_{x\text{-}An}$ was prepared by using [DBS] = 1×10^{-4} M. The two images show similar features and size of the NiO_x particles. Semispherical shape with an average size of the particles of ~ 80 nm are obtained. It may be concluded that the difference in electrochemical activity of the GC/NiO_x (A) and GC/$NiO_{x\text{-}An}$ is due to adsorption of the DBS onto the NiO_x particles in case of GC/$NiO_{x\text{-}An}$. The latter adsorption process may facilitate the adsorption of the glucose molecules on the electrode surface (GC/$NiO_{x\text{-}An}$) leading to higher rates of the glucose electrochemical oxidation reaction.

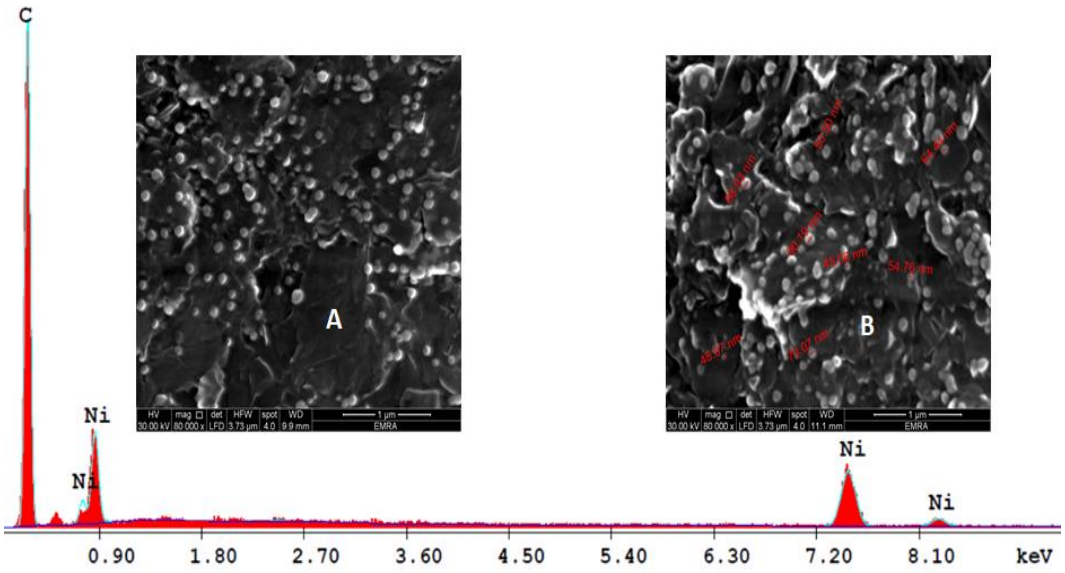

Figure 5. SEM images of the GC/NiO_x (A) and GC/$NiO_{x\text{-}An}$ (B) and the EDX chart.

Figures 6A, B depict the CV responses of GC/NiO_x and GC/$NiO_{x\text{-}An}$, respectively at different scan rates using 20 mM glucose in 0.5 M NaOH. As the scan rate, ν increases the peak current increases. At scan rate > 100 mV s^{-1}, thecathodic peak of the conversion, $NiOOH \rightarrow Ni(OH)_2$ becomes more obvious in case of the GC/$NiO_{x\text{-}An}$ electrode (Fig. 6B). As it was discussed above that the Ni^{2+}/Ni^{3+} transform is faster than on GC/$NiO_{x\text{-}An}$. As discussed in Figs. 2 and 3, the concentration of the nickel species in case of GC/$NiO_{x\text{-}An}$ is higher than that of GC/NiO_x. Consequently, the cathodic peak of the conversion $Ni^{3+} \rightarrow Ni^{2+}$ appears in the cathodic sweep on the GC/$NiO_{x\text{-}An}$ electrode. Figure 6C represents the plot of $I_p/\nu^{0.5}$ with the scan rate, ν for glucose electrooxidation from 20 mM glucose in 0.5 M NaOH on GC/NiO_x (A) and GC/$NiO_{x\text{-}An}$ (B), respectively. The features of the curves A and B are the characteristics for electrocatalytic oxidation process. Note that at lower scan rates there are larger differences between the peak currents of GC/$NiO_{x\text{-}An}$ than on GC/NiO_x. This can be discussed in

the light of the larger amount of redox species NiOOH and $Ni(OH)_2$ (see Fig. 1) and hence a lower scan rates are needed for glucose oxidation to consume all the available NiOOH. The above enhancement of electrocatalytic activity of Ni-based electrocatalysts have been observed also in literatures [35-37]. For instance, Hu et al. found greater electrocatalytic oxidation of hydrodehalogenation of 2,4-dichlorophenol on Ni-based catalyst prepared in presence of surfactant [38]. The effect of sodium dodecyl sulfate on electrocatalytic characterizations of PPAA/Ni modified electrode toward electrocatalytic oxidation of ethylene glycol [39].

By considering some literatures for studying the mechanisms of glucose oxidation on Ni-based electrocatalysts [40-46], two possible mechanisms for the electrooxidation of glucose molecules on the NiOOH catalyst in alkaline medium were proposed. One is the direct oxidation and the other is indirect or catalyst regeneration (EC$'$) mechanism. In the direct oxidation mechanism glucose is oxidized on the NiOOH electrode surface (Eqs. (2) and (3)). Several studies discussed the possible mechanisms and accordingly the direct mechanism is still valid at the prevailed conditions can be given by; [40-46]

Ni(III)-glucose → Ni(III)-intermediate (2)

Ni(III)- intermediate → Ni(III)-products (3)

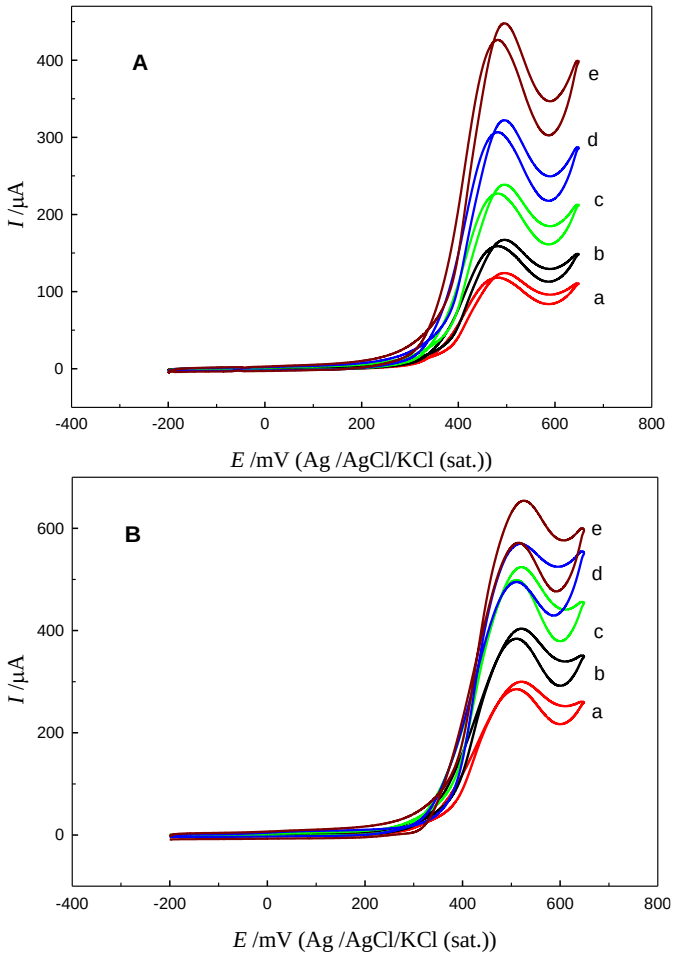

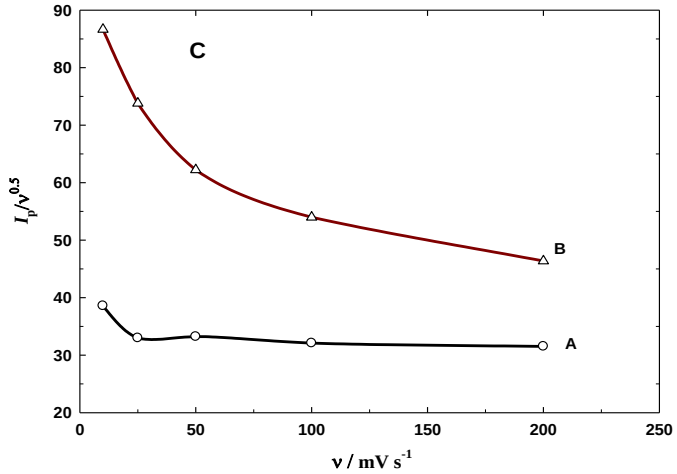

Figure 6. The effects of potential scan rate, ν on the CV response of the GC/NiO_x (A) and GC/$NiO_{x\text{-}An}$ (B) electrodes in 0.5 M NaOH containing 20 mM glucose solution (ν: 10. 25, 50, 100 and 200 mV s^{-1}). (C) A plot $I_p/v^{0.5}$ the scan rate, ν (A: GC/$NiO_x$and B: for GC/$NiO_{x\text{-}An}$).

The indirect oxidation or catalyst regeneration (EC') mechanism of glucose on NiOOH catalyst is shown below [40-46]. Accordingly, $Ni(OH)_2$ is electrochemically oxidized to NiOOH and then the

catalytically active NiOOH is chemically reduced to the inactive $Ni(OH)_2$ by glucose oxidation. Meanwhile, glucose is chemically oxidized to products. The inactive $Ni(OH)_2$ will be electrochemically oxidized to NiOOH due to the prevailing high oxidation potential thus regenerating the catalyst for further oxidation of glucose molecules. This can be given by;

$$Ni(OH)_{2(s)} + OH^- \rightleftarrows NiOOH_{(s)} + H_2O_{(l)} + e^- \quad (4)$$

$$NiOOH_{(s)} + \text{glucose}_{(aq)} \rightarrow Ni(OH)_{2(s)} + \text{products} \quad (5)$$

The above two equations imply the catalyst regeneration as per the indirect oxidation of glucose. Gluconolactone as well as methanoates and oxalates have been reported as the oxidation products of glucose electrooxidation [40-45].

Tafel plots for both GC/NiO_x (A) and GC/$NiO_{x\text{-}An}$ (B) are given in Fig. 7 (A and B) at scan rate of 5 mV s^{-1}. The above results show an increase in the activity of the glucose oxidation on the GC/$NiO_{x\text{-}An}$ compared to GC/NiO_x. Tafel slopes calculated from the above figures to be 120 and 131 mV dec^{-1} for GC/NiO_x and GC/$NiO_{x\text{-}An}$, respectively. This may imply a similar mechanisms of the analyte oxidation on both electrodes and hence it is controlled by one-electron step (see Eq. 3).

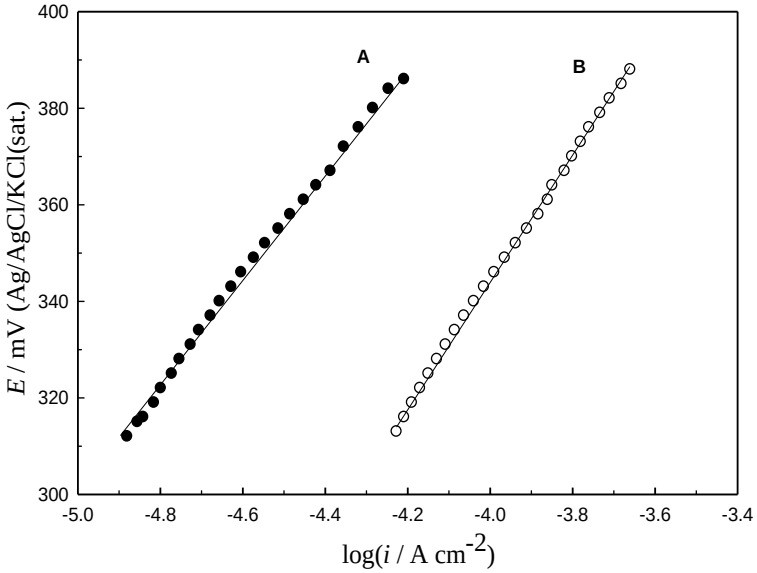

Figure 7. Tafel plots of A: GC/$NiO_x$and B: for GC/$NiO_{x\text{-}An}$ in 0.5 M NaOH containing 10 mM glucose.

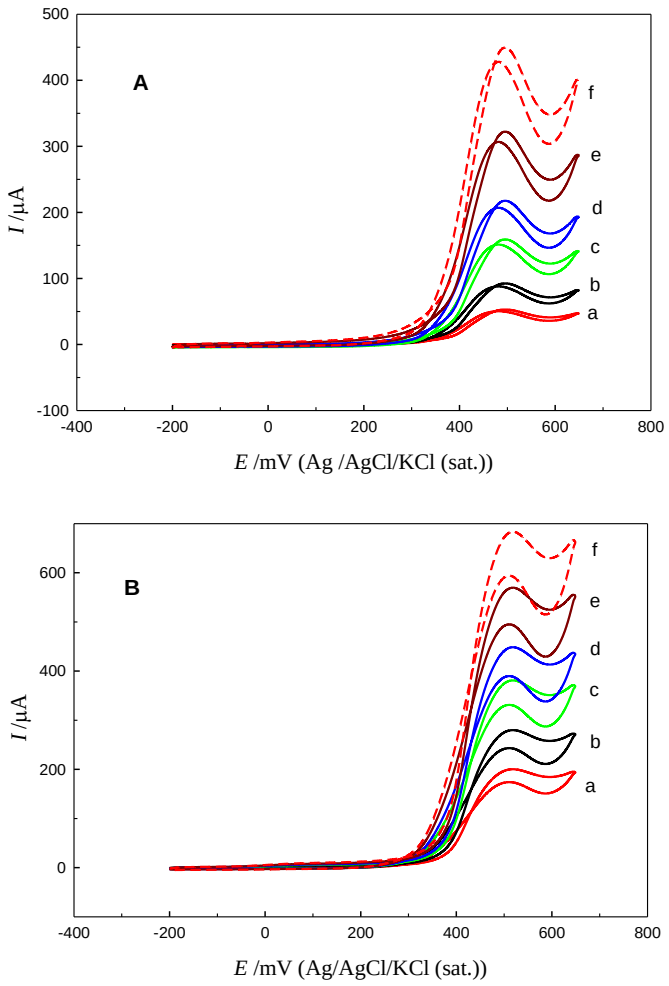

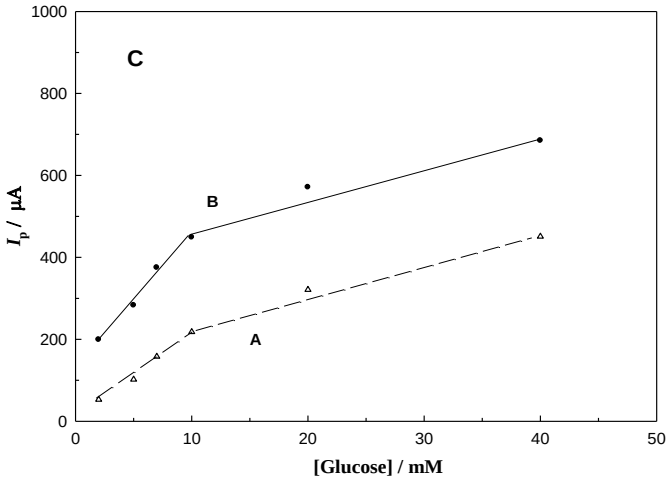

Figure 8. Effect of [glucose] on the CV response of A: $GC/NiO_x$and B: for $GC/NiO_{x\text{-}An}$ at scan rate of 100 mV s^{-1}. (C) I_p of glucose oxidation as a function of [glucose].

Figure 8A and 8B show CV responses for glucose electrooxidation at scan rate 100 mV s^{-1} from different glucose concentrations in 0.5 M NaOH on GC/NiO_x, and $GC/NiO_{x\text{-}An}$, respectively. As the [glucose] increases, the peak current increases and the onset potential of glucose electrooxidation shifts to more negative values. This demonstrates that glucose oxidation is a diffusion-controlled process on both electrodes. A plot of I_p with the [glucose] is given in Fig. 8C for GC/NiO_x(a), and $GC/NiO_{x\text{-}An}$ (b), respectively. A reasonable straight line is obtained up to [glucose] = 10 mM on both electrodes which indicates a diffusion-controlled process. The sensitivity of $GC/NiO_{x\text{-}An}$ electrode to glucose concentrationis higher (higher slope) than that of GC/NiO_x. The peak current for glucose oxidation on $GC/NiO_{x\text{-}An}$ is higher than that obtained on the GC/NiO_x electrode which confirms the above conclusion of the better electroactivity of the $GC/NiO_{x\text{-}An}$, towards electrocatalytic oxidation of glucose.

4. CONCLUSIONS

Nickel oxide nanoparticles were fabricated in presence of different concentrations of anionic surfactant (DBS) on a GC electrode. In presence of the DBS during nickel deposition, the NiO_x nanoparticles revealed enhancement of the electrochemical properties. The activity and reversibility of $GC/NiO_{x\text{-}An}$ in blank 0.5 M NaOH is better than of GC/NiO_x. The impacts of the above modification on the electrooxidation of glucose as a probe reaction were studied. Optimum concentration of DBS of 10^{-4} M was found to give the best activity of $GC/NiO_{x\text{-}An}$ in blank (0.5 M NaOH) and in presence of glucose. The SEM images and electrochemical characteristics enabled to discuss the above impacts.

ACKNOWLEDGEMENT
This work was supported by the grants from the Deanship of Scientific Research, King Faisal University (project # 130186). The financial contribution is gratefully acknowledged. The authors also thank the Department of Chemistry, College of Science, King Faisal University for getting this article published.

References

1. M. A.Malik, M. A. Hashim, F. Nabi, S. A. AL-Thabaiti, Z. Khan, *Int. J. Electrochem. Sci.*, 6 (2011) 1927.
2. R. Vittal, H. Gomathi, K.-J Kim, *Adv. Colloid Interface Sci*., 119 (2006) 55.
3. D. A. C. Brownson, J. P. Metters, D. K. Kampouris, C. E. Banks, *Electroanalysis*, 23 (2011) 894.
4. A. Khamis, M. M. Saleh, Mohamed I. Awad, B.E. El-Anadouli, *Corros. Sci*., 74 (2013) 83.
5. G.Yasin, M. Arif, M. N. Nizam, M. Shakeel, M. A. Khan, W. Q. Khan, T. M. Hassan, Z. Abbas, I. Farahbakhsh, Y. Zuo, *RSC Adv.*, 8 (2018) 20039.
6. J. Melke, D. Dixon, L. Riekehr, N. Benker, J. Langner, C. Lentz, H. Sezen, A. Nefedov, C. Woll, H. Ehrenberg, C. Roth, *J. Catal*., 364 (2018) 282.
7. D. Xu, Y. Liu, S. Zhao, Y. Lu, M. Han, J. Bao, *Chem. Commun*., 9 (2018) 4451.
8. K.C. Pillai, G. Muthuraman, Il-Shik Moon, *J. Colloid Interface Sci*., 512 (2018) 871.
9. Y.-P Wu, W. Zhou, J. Zhao, W.-W Dong, Y.-Q Lan, D.-S. Li, C. Sun, X. Bu, *Angew. Chem., Int. Ed*., 56 (2017) 13001.
10. W. Wang, K. Zhang, Z. Qiao, L.Li, P. Liu, Y. Yang, *Ind. Eng. Chem. Res*., 53 (2014) 10301.
11. X. Duan, F. Ma, Z. Yuan, L. Chang, X. Jin, *J. Electroanal. Chem*., 677–680 (2012) 90.
12. N. Hassanzadeh, H. R. Z.-Mehrjardi, *Int. J. Electrochem. Sci*., 12 (2017) 3950.
13. X. Wang, I-Ming Hsing, *Electrochim. Acta*, 47 (2002) 2981.
14. P.B. Deroco, B. C. Lourencao, O. F.-Filho, Microchem. J., *in press* (2108).
15. W. Xing, F. Li, Z. Yan, G. Lu, *J. Power Sources* 134 (2004) 324.
16. Mao-Sung Wu, H-Ho Hsieh, *Electrochim. Acta*, 53 (2008) 3427
17. G. Snook, N. Duffy, A. Pandolfo, *J. Electrochem. Soc*., 155 (2008) A262.
18. Su-Juan Li, Wei Guo, Bai-Qing, Yuan Dao-Jun, Zhang Zhu-Qing, Feng Ji-Min Du, *Sens. Actuators*, B, 240 (2017) 398.
19. C.-Yu Lin, Y.-ChienChueh, C.-Hsien Wu, *Chem. Commun*., 53 (2017) 7348.
20. Y. Hu, J. Jin, P. Wu, H. Zhang and C. Cai, *Electrochim. Acta*, 56 (2010) 491.
21. S.-Y. Kwon, H.-D. Kwen and S.-H. Choi, *J. Sensors*, 2012 (2012) 8.
22. S. Hui, J. Zhang, X. Chen, H. Xu, D. Ma, Y. Liu and B. Tao, *Sens. Actuators*, B, 155 (2011) 592.
23. A.M. Ghonim, B.E. El-Anadouli, M.M. Saleh, *Electrochim. Acta* 114 (2013) 713.
24. A.S. Danial, M. M. Saleh, S. A. Salih, M. I. Awad, *J. Power Sources*, 293 (2015) 101.
25. Li, Y. Liu, L. Li, Z. Du, S. Xu, M. Zhang, X. Yin, T. Wang, *Talanta*, 77 (2008) 455 .
26. S. Berchmans, H. Gomathi, G. Prabhakara Rao, *J. Electroanal. Chem*., 394 (1995) 267.
27. L.-C. Jiang, W..D. Zhang, *Biosens. Bioelectron*, 25 (2010) 1402.
28. D. Das, P.K. Sen, K. Das, *Electrochim. Acta* 54 (2008) 289.
29. Y.B. Vasilév, O. A. Khazova, N. N. Nikolaera, *J. Electroanal. Chem*., 196 (1985) 127.
30. Q. Qian, Q. Hu, L. Li, P. Shi, J. Zhou, J. Kong, X. Zhang, W. Huang, *Sens. Actuators*, B, 257 (2018) 23.
31. L. Zhang, Y. Ding, R. Li, C. Ye, G. Zhaoa, Y. Wang, *J. Mater. Chem*. B, 5 (2017) 5549.
32. Da-Un-Jin Jung, R. Ahmad, Y.-B Hahn, *J. Colloid Interface Sci*., 512 (2018) 21.
33. M.M. Saleh, A. A. Atia, *J. Adhes. Sci. Technol*., 17 (1999) 53.
34. J.B. Raoof, M. A. Karimi, S. R. Hosseini, S. Mangelizadeh, *J. Electroanal. Chem*., 638 (2010) 33.
35. Y. Miao, L. Ouyang, S. Zhou, L. Xu, Z.Yang, M. Xiao, R. Ouyang, *Biosens. Bioelectron*., 53 (2014) 428.
36. B. Wu, N. Zheng, *NanoToday*, 8 (2013) 168.
37. Z. Sun, K.Wang, X. Wei, S. Tong, X. Hu, *Int. J. Hydrogen Energy*, 37 (2012) 17862.
38. R. Ojani, J.-B. Raoof, V. Rahemi, *Int. J. Hydrogen Energy*, 36 (2011) 13288.
39. A.L. Rinaldi, R. Carballo, *Sens. Actuators*, B, 228 (2016) 43.
40. S. Wang, C.Wang, G.Wei, H. Xiao, N. An, Y. Zhou, C. An, J. Zhang, *Colloids Surf*., A, 509 (2016) 252.

41. S. Majdi, A. Jabbari, H. Heli, *J. Solid State Electrochem*., 11 (2007) 601.
42. R.H. Tammam, A. H. Touny, Mahmoud M. Saleh, *Environ Sci Pollut Res Int*, 25 (2018) 19898.
43. R.L. Doyle, G. Komarkova, P. O'Brien, M. E. G. Lyons, *ECS Trans*., 53 (16) (2013) 1.
44. R.H. Tammam, A.H. Touny, M. E. Abdesalam, M. M. Saleh, *J. Electroanal. Chem.*, 823 (2018) 128.
45. M. Fleischmann, K. Korinek, D. Pletcher, *J. Electroanal. Chem*., 31 (1971) 39.

© 2019 The Authors. Published by ESG (www.electrochemsci.org). This article is an open access article distributed under the terms and conditions of the Creative Commons Attribution license (http://creativecommons.org/licenses/by/4.0/).